14th International Symposium on Particle Image Velocimetry – ISPIV 2021
August 1–5, 2021

Ultrasound PIV Uncertainty Quantification

R. Derakhshandeh[1*], S. Bhattacharya[1], B. A. Meyers[1], P. P. Vlachos[1]

[1] School of Mechanical Engineering, Purdue University, West Lafayette Indiana, 47907, USA

[*] rderakhs@purdue.edu

Abstract

Ultrasound Particle image velocimetry (UPIV) is a non-invasive flow measurement technique where acoustic-opaque flow tracers are injected into a working fluid and ensonified to create ultrasound images. These images are processed using PIV cross-correlation based algorithms to measure the velocity field (Kim et al., 2004). UPIV is useful for opaque flows, primarily where complex flows exist, accordingly, it is used in many industrial and clinical research applications such as studying intracardiac flow (Crase et al., 2007). Furthermore, the measurement provides suitable temporal and spatial resolutions for improved diagnostic metrics. Mentioned applications and the sensitive diagnostic industrial and clinical decisions made based on these measurements intensifies the importance of characterizing the UPIV measurement accuracy and associated uncertainty. However, quantifying UPIV measurement uncertainty is non-trivial due to the complexity of possible uncertainty sources, their combination, and propagation through the measurement chain.

The formation of a particle image by ultrasound significantly differs from optical imaging, introducing unique aspects to image quality that must be considered. Particle images are formed across several ultrasound scan lines, yielding an elliptical particle image shape. Furthermore, the particle's reflected pressure wave is converted to a digital signal that undergoes signal modulation, and this process forms a non-Gaussian point spread function (PSF) along the scan line direction. Additionally, clusters of tracers produce a single, bright image intensity and speckle image pattern. Compared to conventional PIV images, UPIV incurs significantly higher image noise due to lack of filtration for the ultrasound reflection of the non-tracer obstacles.

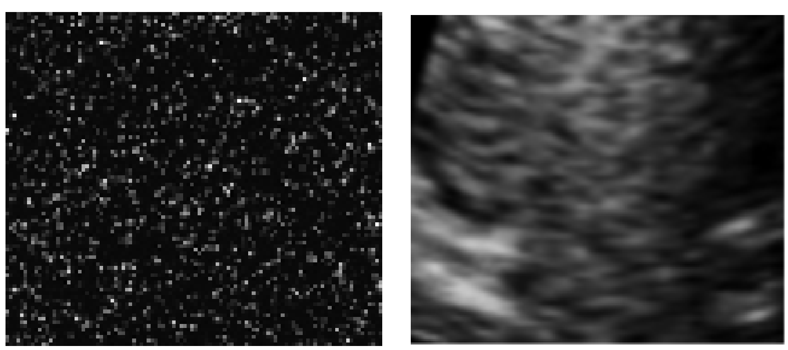

(a) (b)

Figure 1: Comparison of a conventional PIV image(a), and an Echo PIV image(b)(Crase et al., 2007)

Although existing 2D PIV uncertainty methods can potentially be applied to UPIV, the image formation aspects introduced above must be taken into account to quantify UPIV measurement uncertainty. Therefore, in this work, we modified the methodology of three direct uncertainty estimation methods, Image Matching (IM) (Sciacchitano et al., 2013)Moment of Correlation (MC) (Bhattacharya et al., 2018), and Correlation Statistics (CS) (Wieneke, 2015), in order to increase their sensitivity to error sources specific to UPIV. In the following paragraphs, these improvements are explained in detail.

In the IM method, the standard uncertainty is defined as the standard deviation of the disparity error histogram. The disparity error relates to the residual mismatch between paired particle image positions. In regular PIV, the position is estimated using a 3-point Gaussian fit. However, UPIV scans lead to significantly

stretched elliptical particle image patterns with aspect ratios 1 to 4, causing similar pixel intensities in the 3-point neighborhood of the center. Thus, a 3-point fit often fails or is inaccurate. To overcome this limitation, we instead use a least-square elliptic Gaussian fit for particle image position estimation and disparity values to calculate the IM uncertainty.

For the MC method, the uncertainty is estimated directly from the cross-correlation plane by extracting the probability density function (PDF) of the displacements. The standard algorithm assumes a Gaussian PDF exists and convolves it with another circular Gaussian kernel to broaden the peak region. This leads to a more reliable PDF standard deviation estimate. The MC uncertainty calculation uses the sum of the covariance matrices for Gaussian convolution, which simplifies to the sum of the variance terms for a circular Gaussian kernel, expressed as $P_x = \sqrt{C_x^2 - D^2}$ and $P_y = \sqrt{C_y^2 - D^2}$. Here, P_x and P_y are the PDF's major and minor axis, C_x and C_y are the convolved PDF peak diameters, and D is the circular Gaussian kernel diameter. The kernel diameter is dynamically estimated from the cross-correlation peak's width. Since in a UPIV measurement, the cross-correlation peak is non-circular, the convolution kernel is also defined as a non-circular Gaussian function. Thus, a theoretical framework for a generically rotated elliptic Gaussian kernel convolution is deduced. Accordingly, the elliptical Gaussian kernel major axis (D_x), the minor axis (D_y), and the orientation angle (α) are calculated by equations (1), (2), and (3) respectively.

$$P_x^2 = \frac{(C_x^2 + C_y^2) - (D_x^2 + D_y^2) + \sqrt{(C_x^2 - C_y^2)^2 - (D_x^2 - D_y^2)^2 - 2(C_x^2 - C_y^2)(D_x^2 - D_y^2)cos\alpha}}{2} \tag{1}$$

$$P_x^2 = \frac{(C_x^2 + C_y^2) - (D_x^2 + D_y^2) - \sqrt{(C_x^2 - C_y^2)^2 - (D_x^2 - D_y^2)^2 - 2(C_x^2 - C_y^2)(D_x^2 - D_y^2)cos\alpha}}{2} \tag{2}$$

$$\alpha = \frac{(C_x^2 cos^2(\beta) + C_y^2 sin^2(\beta) - D_x^2) - (P_y/P_x)^2 (C_x^2 sin^2(\beta) + C_y^2 cos^2(\beta) - D_y^2)}{P_x^2 - (P_y^4/P_x^2)} \tag{3}$$

In equation (3), β is the orientation of convolved PDF peak obtained from the least square fitting.

The CS method models the uncertainty through the cross-correlation peak's asymmetry attributed to the covariance sum of the pixel-wise intensity difference between two matching interrogation windows. In general, this sum is computed over a neighborhood region proportional to the particle image size. For UPIV measurements, the CS uncertainty calculation is modified to dynamically set the covariance sum region in each direction proportional to the estimated autocorrelation diameter.

The performance of the modified IM, MC, and CS methods are tested using synthetic ultrasound images (Meunier and Bertrand, 1995) that represent a range of error sources, including particle image diameter, noise, seeding density, displacement, and flow shear rate. For the baseline condition, 512×512 images with 3×9 pixel diameter particles are generated with a seeding density of 0.03 particles per pixel with Multiplicative ($\sigma^2 = 0.01$) and additive ($\sigma^2 = 0.01, \mu = 0$) noise and constant displacements of 2.15 pixels in both the x- and y-directions. Also, to consider for the ghost particles, random particles has been added to the images; the number of these random particles is 5% of the total particles. The relevant parameters for the Monte Carlo image simulations are presented in the Table 1. The parameters were varied independently to test each method's sensitivity to different error sources.

Table 1: Monte Carlo test matrix

Diameter Y-direction	3 pixels
Diameter X-direction	3:1:12 pixels
Displacement Y-direction	0:0.05:3 pixels
Displacement X-direction	Same as it is in Y-direction
Shear Y-direction	0
Shear X-direction	0:0.05:015 pixels/frame/pixel
Density	0.01:0.005:0.05
Additive noise	0:0.01:0.1
Multiplicative noise	0:0.01:0.1

Figure 2 shows the RMS error and the RMS of the predicted uncertainty for each method as a function of particle image aspect ratio (AR). The particle image aspect ratio varies from 1 to 4 by varying the x-direction image diameter from 3 to 12 pixels, and the y-direction image diameter is kept constant at 3 pixels. Each point in the plot represents the RMS value over 12800 measurements. For ideal prediction, the RMS of the error distribution should match the RMS of the uncertainty distribution (Sciacchitano et al., 2015).

The current results show close agreement between the predicted and expected IM uncertainty values for up to 1.5 AR. MC uncertainty predictions are within 10% of the RMS error between AR values 1 and 2. All three methods' performance deteriorates for AR values greater than 3, signifying further development may be required to account for the specific particle image characteristics in UPIV. Further development and validation will be done to improve each method's performance to the different error sources.

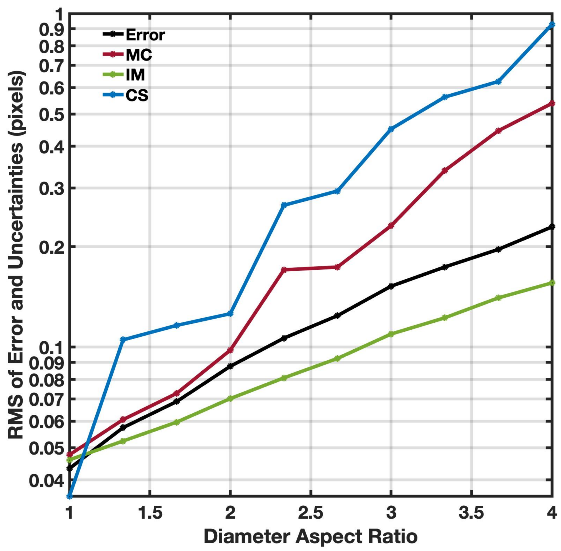

Figure 2: Comparison of the uncertainty methods results over different particle aspect ratio

References

Bhattacharya S, Charonko JJ, and Vlachos PP (2018) Particle image velocimetry (piv) uncertainty quantification using moment of correlation (mc) plane. *Measurement Science and Technology* 29:115301

Crase SJ, Hockaday C, and McCarville PC (2007) Brief report: Perceptions of positive and negative support: Do they differ for pregnant/parenting adolescents and nonpregnant, nonparenting adolescents?. *Journal of Adolescence* 30:505–512

Kim HB, Hertzberg JR, and Shandas R (2004) Development and validation of echo piv. *Experiments in fluids* 36:455–462

Meunier J and Bertrand M (1995) Echographic image mean gray level changes with tissue dynamics: a system-based model study. *IEEE Transactions on Biomedical Engineering* 42:403–410

Sciacchitano A, Neal DR, Smith BL, Warner SO, Vlachos PP, Wieneke B, and Scarano F (2015) Collaborative framework for piv uncertainty quantification: comparative assessment of methods. *Measurement Science and Technology* 26:074004

Sciacchitano A, Wieneke B, and Scarano F (2013) Piv uncertainty quantification by image matching. *Measurement Science and Technology* 24:045302

Wieneke B (2015) Piv uncertainty quantification from correlation statistics. *Measurement Science and Technology* 26:074002